Conversion to stem-cell state in response to microenvironmental cues is regulated by balance between epithelial and mesenchymal features in lung cancer cells

*Francesca Andriani[a,1], Giulia Bertolini[a,1], Federica Facchinetti[a], Erika Baldoli[a], Massimo Moro[a], Patrizia Casalini[b], Roberto Caserini[a], Massimo Milione[c], Giorgia Leone[d], Giuseppe Pelosi[d], Ugo Pastorino[e], Gabriella Sozzi[a,**], Luca Roz[a,*]*

[a]*Tumor Genomics Unit, Department of Experimental Oncology and Molecular Medicine, Fondazione IRCCS Istituto Nazionale dei Tumori, Milan, Italy*
[b]*Molecular Targeting Unit, Department of Experimental Oncology and Molecular Medicine, Fondazione IRCCS Istituto Nazionale dei Tumori, Milan, Italy*
[c]*Anatomic Pathology Unit1, Department of Pathology and Laboratory Medicine, Fondazione IRCCS Istituto Nazionale dei Tumori, Milan, Italy*
[d]*Anatomic Pathology Unit2, Department of Pathology and Laboratory Medicine, Fondazione IRCCS Istituto Nazionale dei Tumori, Milan, Italy*
[e]*Thoracic Surgery Unit, Department of Surgery, Fondazione IRCCS Istituto Nazionale dei Tumori, Milan, Italy*

ARTICLE INFO

ABSTRACT

Cancer cells within a tumor are functionally heterogeneous and specific subpopulations, defined as cancer initiating cells (CICs), are endowed with higher tumor forming potential. The CIC state, however, is not hierarchically stable and conversion of non-CICs to CICs under microenvironment signals might represent a determinant of tumor aggressiveness. How plasticity is regulated at the cellular level is however poorly understood. To identify determinants of plasticity in lung cancer we exposed eight different cell lines to TGFβ1 to induce EMT and stimulate modulation of CD133$^+$ CICs. We show that response to TGFβ1 treatment is heterogeneous with some cells readily switching to stem cell state (1.5–2 fold CICs increase) and others being unresponsive to stimulation. This response is unrelated to original CICs content or extent of EMT engagement but is tightly dependent on balance between epithelial and mesenchymal features as measured by the ratio of expression of *CDH1* (E-cadherin) to *SNAI2*. Epigenetic modulation of this balance can restore sensitivity of unresponsive models to microenvironmental stimuli, including those elicited by cancer-associated fibroblasts both *in vitro* and *in vivo*. In particular, tumors with increased prevalence of cells with features of partial EMT (hybrid epithelial/mesenchymal

phenotype) are endowed with the highest plasticity and specific patterns of expression of SNAI2 and CDH1 markers identify a subset of tumors with worse prognosis. In conclusion, here we describe a connection between a hybrid epithelial/mesenchymal phenotype and conversion to stem-cell state in response to external stimuli. These findings have implications for current endeavors to identify tumors with increased plasticity.

1.　　Introduction

Tumors are increasingly recognized as heterogeneous entities characterized by both constantly evolving clones with different genetic alterations (genetic heterogeneity) and cellular subpopulations with distinct phenotypes (functional heterogeneity), including cells with increased tumor forming potential operationally defined as cancer initiating cells or CICs (Burrell et al., 2013; Meacham and Morrison, 2013). A better understanding of the contribution of different mechanisms underlying tumor heterogeneity together with the appraisal of the influence of the tumor microenvironment is needed to gain a better insight on tumor evolution and possibly to devise better therapies (Kreso and Dick, 2014). Modulation of tumor phenotypes is in fact a consequence of genetic and epigenetic changes in the cancer cells combined with their bi-directional interaction with the surrounding microenvironment (Hanahan and Coussens, 2012; Tam and Weinberg, 2013).

From the functional point of view, one hypothesis explaining the nature of heterogeneity is that neoplastic progression is driven by a small subpopulation of cells defined as "cancer initiating cells" (CICs), which are able to guide tumor growth, survive chemotherapy and establish distant metastases (Mueller et al., 2010; Visvader and Lindeman, 2008; Zhou et al., 2009). This subpopulation has the potential to give rise to the entire observed heterogeneous lineages contained in the tumor bulk. A reverse process by which more differentiated progenitors can switch to CICs phenotype has been also described, suggesting an extra layer of complexity imposed by cellular plasticity (Marjanovic et al., 2013). Different mechanisms were proposed to clarify the dynamic phenotypic switch: CICs may be derived by spontaneous conversion modeled as a stochastic process in which cancer cells convert randomly in the different states (Chaffer et al., 2011; Gupta et al., 2011) or may be originated by conversion of non-CICs to CICs, driven by external stimuli including inducers of epithelial-mesenchymal transition (EMT) (Mani et al., 2008). The ability of cancer epithelial cells to invade and disseminate is in fact supported by the highly coordinated EMT process (Polyak and Weinberg, 2009; Thiery et al., 2009) and is characterized by a disorganization of the cytoskeleton, loss of cell−cell adhesion complexes and acquisition of mesenchymal traits. At the molecular level, under appropriate stimuli (i.e. TGFβ1) (Peinado et al., 2007), the EMT process results in coordinated activation of key transcription factors inducing mesenchymal features, including Snail homologues (SNAI1, SNAI2), TWIST and Zinc finger E box-binding homeobox 1 and 2 (ZEB1, ZEB2) and down regulation of epithelial markers, including E-cadherin (Lamouille et al., 2014). In lung cancer Snail family members and in particular SNAI2 transcription factor has been shown to represent one of the major master regulators of EMT induction (Shih and Yang, 2011). Epigenetic mechanisms, including histone modifications and DNA methylation, have been also implicated in altering gene expression during the induction and maintenance of EMT and in coordinating cellular processes that contribute to epithelial-mesenchymal plasticity (Chaffer et al., 2013; Cieslik et al., 2013; Lim et al., 2013). Moreover multiple signaling pathways such as those regulated by NF-kb, WNT/β-catenin, Hedgehog and Notch are strongly implicated in the regulation of the EMT process (Gonzalez and Medici, 2014). On the other hand miR-200 family members have been involved in the inhibition of EMT, invasion and metastasis by down-regulating ZEB family members and stabilizing E-cadherin expression (Ceppi et al., 2010; Korpal et al., 2008). In particular it has been demonstrated that enforced expression of the miR-200 alone is sufficient to prevent TGFβ1-induced EMT in normal epithelial cells (Gregory et al., 2008).

While often associated with induction of EMT, the molecular bases and specific determinants of conversion of non-CICs to CICs have however remained elusive. Recently, ZEB1 has been identified as critical mediator of this process in breast cancer with the demonstration that poised chromatin configuration at the ZEB1 promoter is linked to differential ability of more aggressive (basal) breast cancer cells to generate de novo CICs under microenvironmental stimuli, compared to less aggressive (luminal) subtype (Chaffer et al., 2013). These findings also underscore the importance of cancer cells plasticity in shaping tumor aggressiveness and the possible relevance for therapeutic intervention (Easwaran et al., 2014).

To understand how signals from the microenvironment (ME) could influence the modulation of CICs, we selected a panel of lung cancer cell lines derived from various histological subtypes and with different epithelial/mesenchymal phenotypic characteristics and exposed them to external stimuli including TGFβ1, treatment with medium conditioned by cancer-associated fibroblasts (CAF) and co-injection with CAFs in immunocompromised mice. We found that the extent of response to ME stimuli in the different cell lines both in vitro and in vivo is strictly dependent on the ratio between epithelial and mesenchymal features as estimated by the expression levels of E-cadherin (CDH1) and SNAI2. In particular the frequency of cells co-expressing both markers appears responsible for phenotypic plasticity. In clinical samples of NSCLC, a specific pattern of expression of both proteins identifies cancers with different phenotypic characteristics and is

associated with worst prognosis. This quantitative model provides new insights into how dynamic transitions among epithelial and mesenchymal states can determine the plasticity of cancer cells and modulate lung cancer aggressiveness by enabling CICs formation in response to ME stimuli.

2. Materials and methods

2.1. Cell lines and reagents

Five human NSCLC cell lines were purchased from the American Type Culture Collection (ATCC, LGC Standards): A549, Calu-1, Sk-Mes-1 (SkMes), NCI-H460 (H460), NCI-H1299 (H1299). Three additional primary human NSCLC cell lines were established in our laboratory: LT73, LT215 and LT259. Genomic status of commercial cell lines was retrieved from the Catalogue of Somatic Mutations in Cancer (COSMIC) database of the Wellcome Trust Sanger Institute (www.sanger.ac.uk/cosmic), while primary cancer cells were characterized in our laboratory. Cell lines were maintained in RPMI 1640 (Lonza) supplemented with 10% fetal calf serum (FCS), penicillin (25 units/mL) and streptomycin (25 units/mL). To obtain sphere cultures, cells were plated at a density of 10^4 cells per milliliter in serum-free medium DMEM/F12 (Lonza), supplemented with commercial hormone mix B27 (Gibco), EGF (20 ng/mL; PeproTech), bFGF (10 ng/mL; PeproTech), and heparin (2 μg/mL; PeproTech). Floating sphere cultures were expanded by mechanical dissociation, followed by re-plating of single cells in complete fresh medium every 3 days.

Primary fibroblasts cell lines were obtained from dissociated surgical tissue from primary lung cancer patients (see below), and cultured in Fibroblasts Basal Medium (FBM) supplemented with Fibroblast Growth Kit–Low Serum (ATCC, LGC Standards). For preparation of conditioned medium, fibroblasts (1×10^6) were cultured in Keratinocyte Serum Free Medium (KSFM, Gibco) for 20 h. TGFβ1 (PeproTech) treatment was performed at 5 ng/ml for 3 days. IGFII recombinant protein (Gibco, Life Technologies) was used at 1 ng/ml. TGFβ1 and IGFII neutralizing antibodies (clone #9016 and catalog #AF-292-NA respectively, R&D Systems) were used at 0.5 μg/ml.

To avoid culture conditions artifacts that could influence the correct determination of $CD133^+$ cells, all cell lines were routinely tested for mycoplasma contamination, were grown as adherent monolayers under serum-containing conditions and harvested at controlled density. For miRNA experiments cells were transfected with 50 nmol/L (nM) control-miR (scrambled) or pre-miR-200c (Ambion) with Lipofectamine 2000 reagent (Invitrogen). The minimum effective concentration determined by titration of pre-miR-200c was 5 nM. 5-aza-2'-deoxycytidine (Sigma Aldrich) was used at 5 μM.

2.2. Quantitative real time PCR and RES index quantification

RNA isolation was performed with RNAeasy Kit (Qiagen). Expression levels of EMT-related genes (SNAI2, FN1, VIM, ZEB1, CDH1) and miR-200c were determined by Real-Time PCR using TaqMan® assays (Life technologies) and normalized using the $2^{-\Delta\Delta Ct}$ method relative to HPRT (mRNAs) and RNU48 (miRNAs), respectively. Results are expressed as mean ± SD.

For calculation of "RES index" (Ratio between E-cadherin and SNAI2 expression) the Ct values of both CDH1 and SNAI2 were normalized to relative endogenous housekeeping control (HPRT) and the ratio between expression of CDH1 and SNAI2 (RES index) was evaluated using the formula:

$$\text{Ratio} = 2^\wedge - (Ct_{CDH1} - Ct_{HPRT})/2^\wedge - (Ct_{SNAI2} - Ct_{HPRT}).$$

Considering that Cts of endogenous control are identical within the same sample the formula could be simplified as: $2^\wedge - (Ct_{CDH1} - Ct_{SNAI2})$.

2.3. Tissue dissociation

Clinical specimens were obtained from a consecutive series of consenting patients undergoing surgery for primary lung cancer. The protocol was approved by the Internal Review and Ethics Board of the Fondazione IRCCS, Istituto Nazionale dei Tumori (Milan, Italy). Surgical tissue was finely minced using a scalpel blade, enzymatically digested for 1 h at 37 °C with Tumor Dissociation Kit (Miltenyi Biotec) in the Gentle Macs Octo Dissociator (Miltenyi Biotec) and filtered through a 100 μm cell strainer (BD Falcon). Red blood cells were removed by Lysing Buffer 1X (Becton Dickinson). The obtained suspension was cultured in vitro in RPMI (10% FCS) generally resulting in outgrowth of human fibroblasts. In few instances growth of primary cancer cells was obtained resulting in the generation of LT73, LT215 and LT259 models.

To evaluate dissemination to lungs from subcutaneous tumors, lungs from tumor-bearing mice were digested using the same conditions; human tumor cells in the lungs were identified using a negative gating strategy to exclude 7-AAD+ (non-viable) cells and mouse H2K + cells. This approach was able to specifically detect as few as 10^3 single tumor cells in murine lungs (Bertolini et al., 2015). Cells from suspensions were also plated in vitro and observed to detect the growth of the human cancer cells and verify the specificity of the flow-cytometry assay.

2.4. Flow cytometry analysis

Cell suspensions were washed and incubated in staining solution containing BSA1% and EDTA 2 mM with specific antibodies at appropriate dilution as indicated by datasheets: PE anti-human CD133/1 (clone AC133, Miltenyi Biotec, dilution 1:10) was used to detect lung CICs and PerCP-eFluor 710 anti-mouse MHC class I (E-bioscience, dilution 1:50) for gating of mouse cells in digested murine lungs. 7-AAD viability staining solution (7-Amino-Actinomycin D, E-bioscience, dilution 1:10) was used as a vitality probe for non-viable cell exclusion.

LT73 cells and H460 cells were stained with PE anti-human CD133/1 and sorted for CD133 negative population using BD FACS Aria™ cell sorter.

2.5. Immunofluorescence

Cells were fixed with PFA 4%, permeabilized with Triton X-100 0.15%, blocked with BSA2% +NGS (normal goat serum) 5% solution for 60 min and then double immunostained with anti E-

Cadherin (BD Transduction Laboratory, dilution 1:50) and SNAI2 antibodies (Cell Signaling, dilution 1:400) for 1 h at RT. The secondary antibodies were goat anti-mouse Alexa Fluor 488 and goat anti-rabbit Alexa Fluor 546 respectively. Nuclei were visualized with the VECTASHIELD Mounting Medium, containing DAPI nuclear staining (Vector Laboratories). Imaging was performed using a confocal laser scanning microscope Leica TCS SP8 X (Leica Microsystems GmbH, Mannheim, Germany). The fluorochromes were excited by a continuous wave 405 nm diode laser and a pulsed super continuum White Light Laser (470−670 nm; 1 nm tuning step size). In particular DAPI was excited using diode laser and detected from 410 to 464 nm, AlexaFluor-488 was excited selecting 499 nm-laser lines and detected from 504 to 550 nm and AlexaFluor-546 was excited with 557 nm-laser line and detected from 566 to 705 nm. The images were acquired in the scan format 512×512 pixel in a Z stack series (step size 0.5 μm) using a HC PL APO 63X/1.40 CS2 oil immersion objective and a pinhole set to 1 Airy unit. The intensity of E-cadherin and SNAI2 fluorescence in a single cell area (expressed in pixels) was calculated by ImageJ software. This value was used to estimate frequency of single cells expressing mainly CDH1 (epithelial), SNAI2 (mesenchymal) or co-expressing both markers (hybrid). For each cell line the ratio of the intensity of the two markers in co-expressing cells was calculated and used as normalization factor. The ratio between CDH1 and SNAI2 intensity in 50−100 single cells was then measured and divided by the normalization factor previously calculated. Values between 0.9 and 1.1 denoted cells with hybrid characteristics (E = M), values higher than 1.1, referred to epithelial (E) cells while, values lower than 0.9, represented mesenchymal (M) cells.

2.6. Animal studies

Experiments were approved by the Ethics Committee for Animal Experimentation of the Fondazione IRCCS, Istituto Nazionale dei Tumori (Milan, Italy) according to EU Directive 2010/63/EU. In vivo experiments were carried out using CD1-Nude female mice, 5−10 weeks old (Charles River Laboratories). Mice were maintained in laminar flow rooms, at constant temperature and humidity. Mice had free access to food and water. For subcutaneous tumorigenic assay viable tumor cells (1×10^5 for LT73 or 5×10^2 for H460 cells), alone or with fibroblasts (1:3 ratio), were s.c. injected into the flank of nude mice with Matrigel (BD Biosciences) in a final volume of 200 μl. At the end of the observation period or when the tumors volume reached at least 300 mm^3, lungs were removed and dissociated for further analysis. In limiting dilution experiments, cancer cells were subcutaneously injected at different doses in SCID mice that were observed for up to 2 months. The frequency of Cancer Initiating Cells was calculated based on tumor take rate using ELDA software (Hu and Smyth, 2009) accessed at http://bioinf.wehi.edu.au/software/elda/.

2.7. Patient samples and immunohistochemistry analysis

A series of 60 patients were diagnosed and surgically treated for lung cancer at the Department of Thoracic Surgery at Fondazione IRCCS, Istituto Nazionale dei Tumori (Milan, Italy) between 2008 and 2012. Formalin-fixed, paraffin-embedded samples were available for all 60 primary tumors. Sections (1.5 μm-thick) were cut from paraffin blocks, deparaffinized in xylene and rehydrated with distilled water. Antigen retrieval was performed in citrate buffer solution (5 mM/L, pH6). After peroxidase inhibition with a solution of 0.3% H_2O_2 in methyl alcohol for 30 min, the slides were incubated with the following antibodies: anti SNAI2 (Cell Signaling) and anti E-cadherin (BD Transduction Laboratory) at the indicated concentration.

The primary antibody detection was performed using Ultra Vision detection system-HPR polymer (Thermo Fisher Scientific, Waltham, MA,USA) and DAB substrate chromogen (Dako), followed by counterstaining with haematoxylin. Tumor sections were scored for the nuclear expression of SNAI2 protein or membrane staining for CDH1. Staining for SNAI2 was evaluated under regular light microscopy by two independent observers, blinded to the clinical data. The staining index was calculated multiplying the percentage of positive stained cells by the specific level of staining intensity (0 = no or low expression, 1 = intermediate intensity, 2 = high intensity). CDH1 staining was classified for cell membrane intensity (MI) in two categories, from an intermediate expression (1) through to an intensive staining (2). Moreover the extension of membrane staining was evaluated as 2 if the membrane was completely stained or 1 if the staining was not complete. The correlation analysis with follow-up was performed combining all these three parameters, SNAI2 score, CDH1 membrane intensity and extension staining. Kaplan−Meier curves were then used to assess the potential prognostic value of SNAI2 and CDH1 on overall survival (OS).

2.8. Statistical analyses

For cell lines experiments, all data are expressed as mean ± SD. Student's t test (two tailed) were used to compare two groups ($p < 0.05$ was considered significant). In vivo tumor growth experiments were analyzed using Kaplan−Meier survival curves estimated by the presence of a tumor lesion above a pre-specified threshold (300 mm^3). p-values were calculated using the log-rank test. The percentage of human tumor cells in murine lung was measured considering viable (7-AAD negative) and negative to anti-mouse MHC class cells population. Differences between groups were calculated with Student's t using GraphPad software version 5.0. In all experiments, statistical significance was set at $p < 0.05$.

To analyze the prognostic potential of SNAI2 or CDH1, patients were grouped according to SNAI2 expression into negative (SNAI2 = 0), intermediate (SNAI2<80) and high expressors (SNAI2>80) where 80 represents the median value of staining intensity, and according to E-cadherin expression into intermediate (MI = 1) and high (MI = 2). Combining the expression of both markers the patients were stratified in 9 groups (as highlighted in Figure 7Ac). Overall patient survival (OS) was defined as the time between the date of surgical diagnosis to the date of last follow-up (censored) or date of patient death (event). Survival probabilities were estimated using the Kaplan−Meier method. p values were calculated using the log-rank test.

3. Results

3.1. *TGFβ1 treatment induces heterogeneous increase of CD133⁺ cancer initiating cells in NSCLC cell lines*

To evaluate the response of lung cancer cells to external stimuli we selected as experimental models eight cell lines from non-small-cell lung cancer (NSCLC) representative of different histological subtypes: five commercial cell lines (A549 from Adenocarcinoma, Calu-1 from Squamous Cell Carcinoma, SkMes from Squamous Cell Carcinoma, H460 from Large Cell Carcinoma, H1299 from Large Cell Carcinoma) and three primary cell lines established in our laboratory (LT73 from Adenocarcinoma, LT215 from Adenocarcinoma and LT259 from Sarcomatoid Carcinoma). To evaluate basal content of cancer initiating cells (CICs) all lines were initially characterized by flow cytometry for the presence of $CD133^+$ cells, previously validated by us and others as a marker of CICs in lung cancer (Bertolini et al., 2009; Eramo et al., 2008). Consistently with earlier reports, flow cytometry analysis showed that expression of CD133 was restricted to a small subpopulation in all cell lines, with a frequency ranging from 0.05% to 0.19% (Figure 1A, Supplementary Figure 1A). The ability of $CD133^+$ CICs to form tumors *in vivo* has been previously extensively investigated by subcutaneous injection in nude mice as the gold standard for the definition of tumor-forming potential. $CD133^+$ cells formed tumors with higher efficiency compared to $CD133^-$ (30 to 1000-fold increase in tumor forming potential) (Bertolini et al., 2009; Eramo et al., 2008) (Supplementary Figure 1B, C). Moreover, we have demonstrated that floating spheres (S) isolated from adherent cell lines (A549, LT73) in a selective serum free medium, are enriched of $CD133^+$ cells (Bertolini et al., 2009) and display higher tumorigenic potential *in vivo* compared to parental counterpart (20-fold increase). Additional results demonstrated that also other cell lines (H1299 and Calu-1) maintained the ability to form floating spheres enriched of $CD133^+$ cells *in vitro* (Supplementary Figure 1D). Despite the highly tumorigenic potential of isolated $CD133^+$ cells, among different cellular models the basal content of $CD133^+$ cells was found not to be directly related to *in vivo* tumorigenic potential (Figure 1B), indicating that modulation of $CD133^+$ cells could have distinct effects in context-specific situations.

Activation of the EMT process by TGFβ1 has been associated with induction of mesenchymal traits and increase of CICs in breast cancer (Mani et al., 2008) and in a primary NSCLC cell line (Pirozzi et al., 2011). To verify whether different tumors respond differently to TGFβ1 with respect to modulation of the CICs compartment, we evaluated the frequency of $CD133^+$ cells after TGFβ1 treatment in the eight NSCLC cell lines with different phenotype. We found that TGFβ1 treatment produced a heterogeneous response with some cell lines showing a relevant increase of $CD133^+$ cells (A549, LT73: more than 1.5 fold increase) while others were only marginally responsive (H460: 1.3 fold increase) or not affected (Figure 1C). The functional relevance of the increase in $CD133^+$ cells was confirmed by a higher *in vivo* tumorigenic potential, with a 4-fold increase in CICs frequency in LT73 cells after TGFβ1 treatment, in line with the observed 2-fold increase in $CD133^+$ cells (Figure 1D).

This differential modulation was not related to the basal content of CD133 and did not appear to depend strongly on the extent of modulation of EMT-related genes (Figure 1E) or on the induction of EMT-related morphological changes (Figure 1F). In particular, modulation of $CD133^+$ phenotype was not strongly correlated with regulation of EMT-related genes which was extremely variable across cell lines (SNAI2 0.96 to 22.5-fold increase, FN1 0.5 to 513-fold increase, ZEB1 0.6 to 2.3-fold increase, CDH1 0.1 to 10-fold decrease). Furthermore, although robust evidence of EMT (both at the transcriptional and morphological level) was generally present in the responsive lines (A549 and LT73), the marginally responsive line H460 did not show strong evidence of EMT and two cell lines unresponsive to $CD133^+$ cells up-regulation (Calu-1 and LT215) were efficiently induced into EMT (Figure 1E and F).

Moreover, responsiveness to external stimuli resulted independent from the tumor histological subtype or from mutations typically present in lung cancer (i.e. p53 or K-ras). Interestingly TGFβ1 induced similar response in generating $CD133^+$ cells regardless of the p53 or K-Ras status being effective in A549 cells (p53 impaired by mutation of p14ARF, K-Ras^{G12S}) and LT73 cells (p53 WT, K-Ras WT). Analogous results were found with regard to cells that are not responsive to TGFβ1 treatment such as Calu-1 (p53 null/K-Ras^{G12C}) or LT215 (p53 WT, K-Ras WT).

3.2. *The acquisition of stemness properties under microenvironmental stimuli depends on the balance of epithelial and mesenchymal features*

To better clarify the association between TGFβ1 stimulation, induction of EMT and the modulation of $CD133^+$ cells, the basal expression levels of EMT-related genes (ZEB1, FN1, VIM, SNAI2 and CDH1) were analyzed. No association was initially observed between response to TGFβ1 and basal expression levels of single EMT-related genes (Figure 2A).

To further investigate the reason for the different responsiveness and thus the proclivity to plasticity we tried to develop a simple index that could provide a rapid classification of the 'phenotypic state' (epithelial/mesenchymal or hybrid) of cell lines to evaluate its relevance in shaping the response to external stimuli in the context of modulation of the stemness phenotype. For their involvement in the EMT process and robust modulation during phenotypic switching we selected CDH1 and SNAI2 as determinants of the epithelial/mesenchymal state and the different lung cancer cell lines were grouped, on the basis of the ratio between expression levels of CDH1/SNAI2 genes (RES index) into "epithelial" (high CDH1, low SNAI2, E⁺), "hybrid epithelial/mesenchymal" (expressing both CDH1 and SNAI2, E > M, E = M or M > E) or "mesenchymal" phenotype (low CDH1 and high SNAI2, M⁺) (Figure 2B). A549 cells showed predominant epithelial phenotype due to high expression of CDH1, but still retained mesenchymal traits (hybrid E > M), LT73 cells were mainly mesenchymal but retained epithelial traits (hybrid, M > E), H460 could be classified as weakly mesenchymal and H1299, Calu-1 and SkMes, LT215 and LT259 displayed increased mesenchymal phenotype (M⁺) (Figure 2B, C). Interestingly, the RES index was found to be predictive of response to TGFβ1 in generating $CD133^+$ cells: A549 and LT73 were more
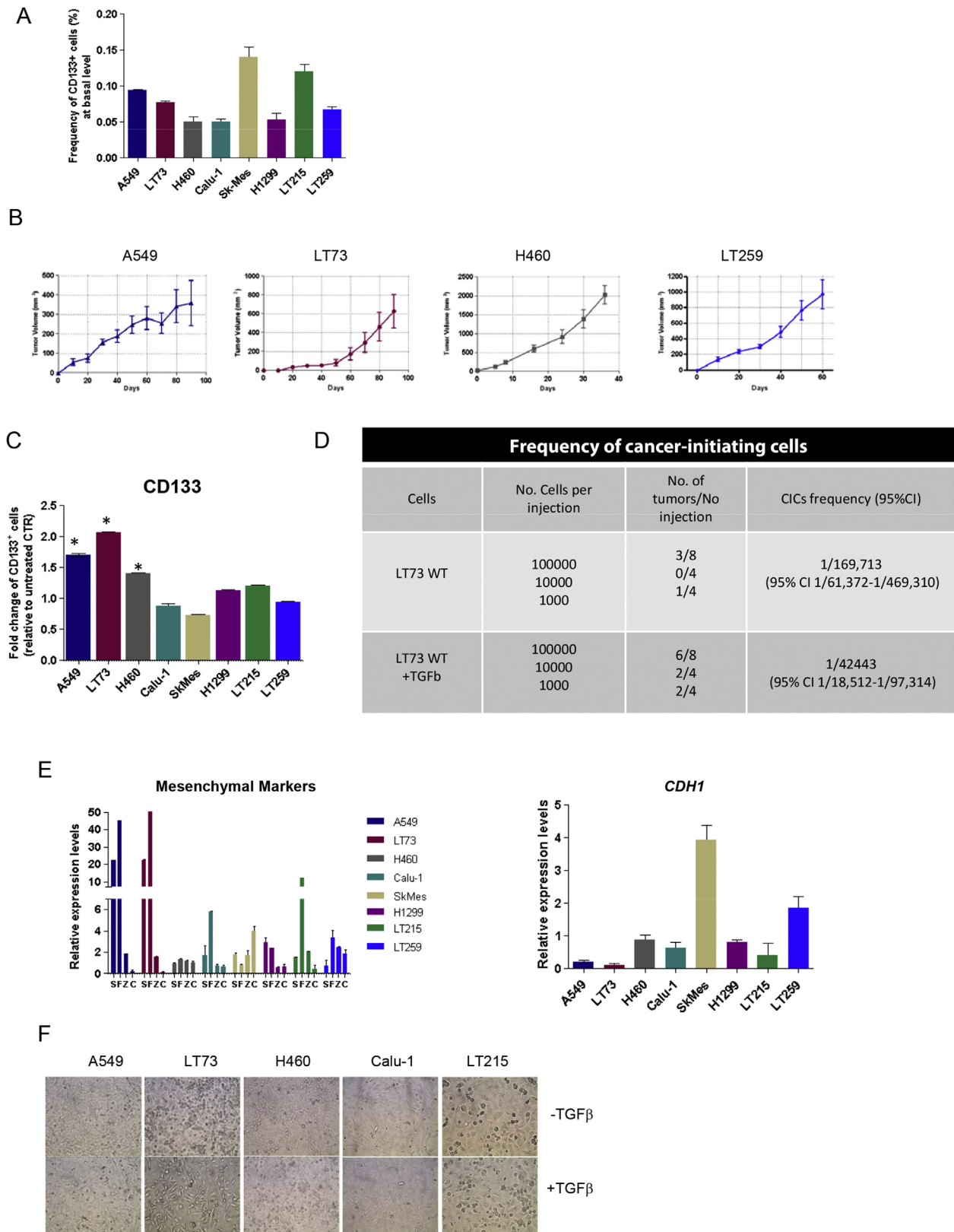
Figure 1 − TGFβ1 induces heterogeneous increase of CD133⁺ CICs in lung cancer cells. (A) Representative analysis by Flow cytometry of CD133 antigen expression in eight different lung cancer cell lines. (B) In vivo tumor growth after s.c injection of 5×10^5 A549, LT73, H460 or LT259 cells into the flanks of nude mice (n = 10 for each cell line). (C) Fold change of CD133⁺ cells after TGFβ1 treatment relative to untreated control. The data represent three independent experiments and replicates are expressed as mean ± SD. *p < 0.05. (D) Effect of TGFβ1 treatment on cancer initiating cells frequency in LT73 cells. Scalar doses of LT73 cells were subcutaneously injected in SCID mice and tumor growth observed for up to two months. (E) Relative expression levels of EMT-related genes after TGFβ1 treatment: S = SNAI2, F = Fibronectin

responsive (1.7 to 2 fold CD133$^+$ cells increase) compared to cells displaying weak mesenchymal properties (H460, 1.3-fold increase) or H1299, Calu-1, SkMes, LT215, LT259 (0.9 to 1.2 fold increase, Figure 1C). These results indicate that a hybrid phenotype could enable lung cancer cell plasticity.

3.3. Phenotypic plasticity can be modulated by epigenetic regulation

To verify the relevance of epithelial/mesenchymal balance in the proclivity to generate CICs under microenvironment stimuli, we then modified the basal phenotype of the different cell lines by ectopic expression of miR-200c (Figure 3A), a known regulator of EMT (Korpal et al., 2008). Transfection of miR-200c induced, as expected, an up-regulation of CDH1: the modulation was marked for all cell lines (10 to 800 fold increase) except for A549 cells (1.3 to 2 fold increase) which already express high basal levels of CDH1. Expression of SNAI2 was relatively unaffected by miR-200c transfection (Figure 3B) thus resulting in an increased RES index. Interestingly, after transfection of miR-200c, A549 cells (A549_miR-200c) displayed exclusively epithelial features (E$^+$, RES>700) "crossing the threshold" of hybrid epithelial cells (E/M). In H460_miR-200c cells, RES index was modified (RES from 0.21) and cells acquired more epithelial features showing a hybrid phenotype (M/E) that was maintained in LT73_miR-200c transfected cell line (RES from 10 to 17). On the other hand, increase of epithelial marker CDH1 in the strongly mesenchymal cell lines, Calu-1, SkMes, H1299, LT215, and LT259 was not sufficient to reach the threshold of hybrid phenotype due to the high expression of mesenchymal features (Figure 3C).

Interestingly, the cell lines that reached the "threshold" of hybrid phenotype acquired (H460_miR-200c) or maintained (LT73_miR-200c) strong sensitivity to external stimuli and generated an enriched CD133$^+$ subpopulation after TGFβ1 treatment. The effect was more evident in the former cells (3.9-fold increase) compared to the latter (2.6-fold increase). Cell lines that did not reach the hybrid threshold and maintained a stronger mesenchymal phenotype did not generate CD133$^+$ cells under TGFβ1 treatment, remaining insensitive to microenvironment stimuli (Figure 3D). Interestingly, however, also the cellular model that "exceeded" the hybrid limit towards more epithelial features (A549_miR200c, E$^+$) lost its responsiveness to ME stimuli and did not generate CD133$^+$ cells after TGFβ1 treatment (Figure 3D). In all cell lines the basal expression of CD133$^+$ cells under miR-200c transfection decreased slightly (data not shown), a phenomenon that could be related to its function as negative regulator of EMT process; however this decrease was not a determinant of the efficacy of TGFβ1 treatment as confirmed by A549 cell line where no evidence of increase was found after treatment.

To determine the minimum concentration of miR-200c able to affect CDH1 levels and modulate RES index (Supplementary Figure 2A and B), we transfected H460 parental cell line with scalar doses of miR-200c (50 nM, 25 nM, 10 nM, 5 nM,1 nM and 0.1 nM) and found 5 nM as minimum concentration required to the cells generate CD133$^+$ cells under TGFβ1 (Supplementary Figure 2C) with a strong correlation between RES index >10 and responsiveness.

The dynamic and reversible changes associated with EMT are connected to a tight epigenetic regulation. In H1299 cell line the promoter region of CDH1 has been demonstrated as being heavily methylated with consequent downregulation of expression (Suzuki et al., 2004). To investigate whether epigenetic modulation could restore the expression of CDH1 allowing a shift of the RES index and affecting the acquisition of stemness phenotype, H1299 cells were treated with demethylating agent 5-aza-2'deoxycytidine alone or in combination with miR-200c. Treatment with 5-aza-2'deoxycytidine alone increased the expression of CDH1 compared to untreated H1299 cells (20-fold increase, Figure 3E). However the modulation of RES index was marginal and insufficient to shift to the hybrid state. Interestingly, the combination treatment of 5-aza-2'deoxycytidine and miR-200c resulted in a synergistic effect in increasing CDH1 expression (500-fold increase, Figure 3E) and in a shift of the RES index above the threshold of mesenchymal traits (RES = 20), reasonably classifying H1299_miR200_AZA as hybrid cells (M > E). Under synergistic treatment, H1299 cells become sensitive to TGFβ1-induced CD133$^+$ cells modulation (1.6-fold increase) compared to untreated control or single treatments (Figure 3F). Together these results provide evidence that epigenetic modulation of epithelial/mesenchymal state of cancer cells could be an important determinant of stemness increase in response to external cues.

3.4. Co-expression of CDH1 and SNAI2 markers identify a small sub-population of cancer cells enabling plasticity

To analyze the possible heterogeneous nature of single cancer cells in the whole cell population, we further investigated whether the two markers were co-expressed to define a specific hybrid sub-population that could confer properties of plasticity in A549, LT73 and H460 parental cell lines. Double immunofluorescence was analyzed by confocal microscope and the analysis was performed with ImageJ software measuring the area of single cells. Considering a field of 100 cells (see Materials and methods), we observed a different frequency of cells expressing epithelial or mesenchymal markers and single cells were classified as mainly epithelial (CDH1^{high}), mesenchymal (SNAI2^{high}) or hybrid (Figure 4A, B). As expected, A549 parental cells contained an elevated frequency of CDH1^{high} cells (82%) and low frequency of SNAI2^{high} cells (7.80%) compared to LT73 parental cells (CDH1^{high} 24% and SNAI2^{high} 47%) or H460 parental cells (CDH1^{high} 19% and SNAI2^{high} 75%). The presence of a hybrid sub-population was more evident in cell lines more responsive to TGFβ1

(FN1), V=Vimentin (VIM), Z = ZEB1 and E-cadherin (CDH1). Expression levels were compared to untreated cells and normalized using HPRT as housekeeping gene. The Real-Time PCR data represent the results of three independent experiments each with three replicates and are represented as mean ± SD. (F) Bright-field microscopy (magnification 40×) of representative cell lines with different phenotypes, before and after 5 ng/ml TGFβ1 for 3 days.
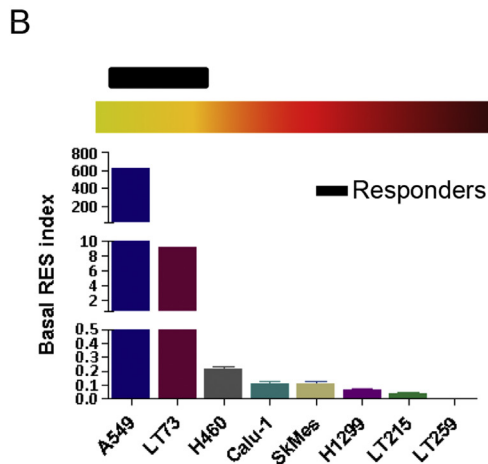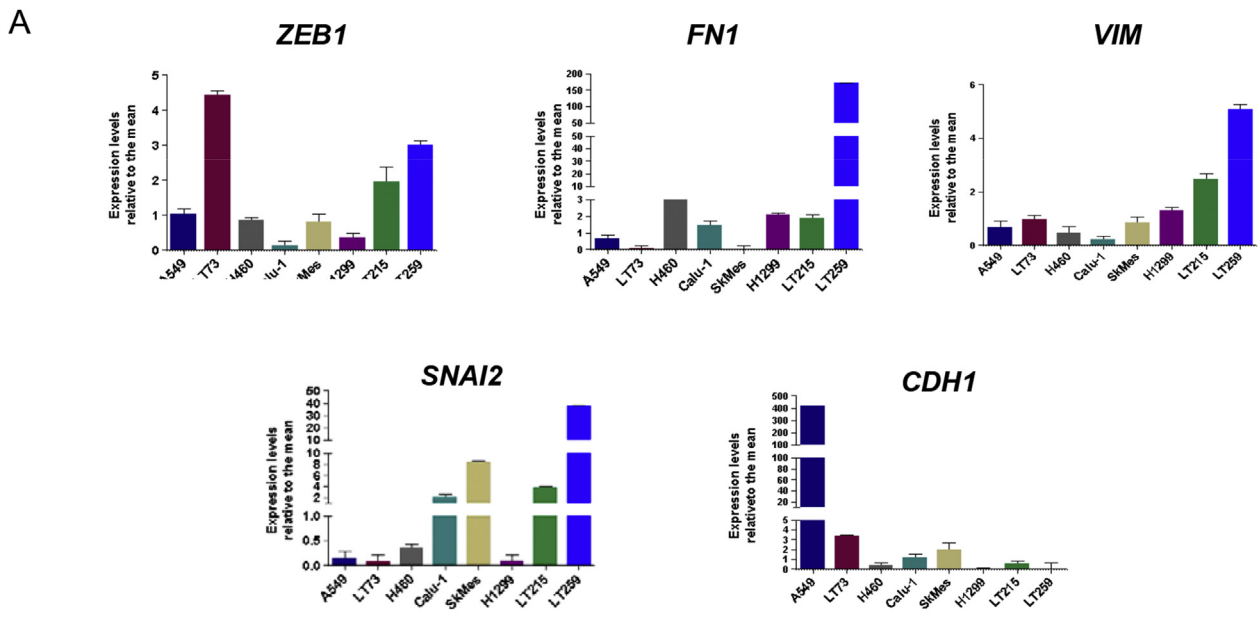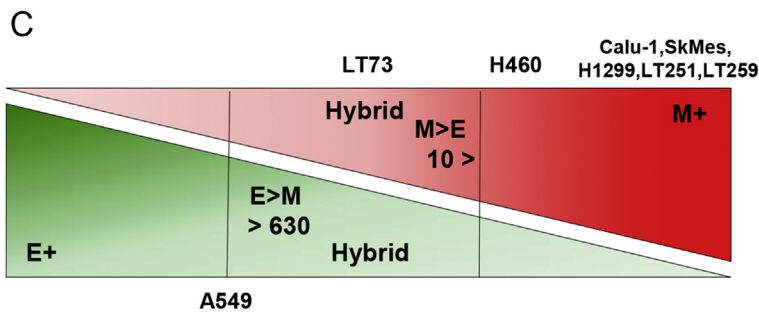
Figure 2 − NSCLC cells display different phenotypic states and can be classified according to the ratio of expression of CDH1 and SNAI2 genes (RES index). (A) Basal expression levels of EMT-related genes analyzed by Real-Time PCR. Average of gene expression of each cell line was used as reference sample. The data are the results of three independent experiments with three replicates each represented as mean ± SD. (B) Alignment of cell lines on the basis of RES index classification. (C) Scheme of different phenotypic state classification of lung cancer cell lines.

Figure 3 − Epigenetic changes regulate cellular plasticity. (A) miR-200c expression levels evaluated by Real-Time PCR (relati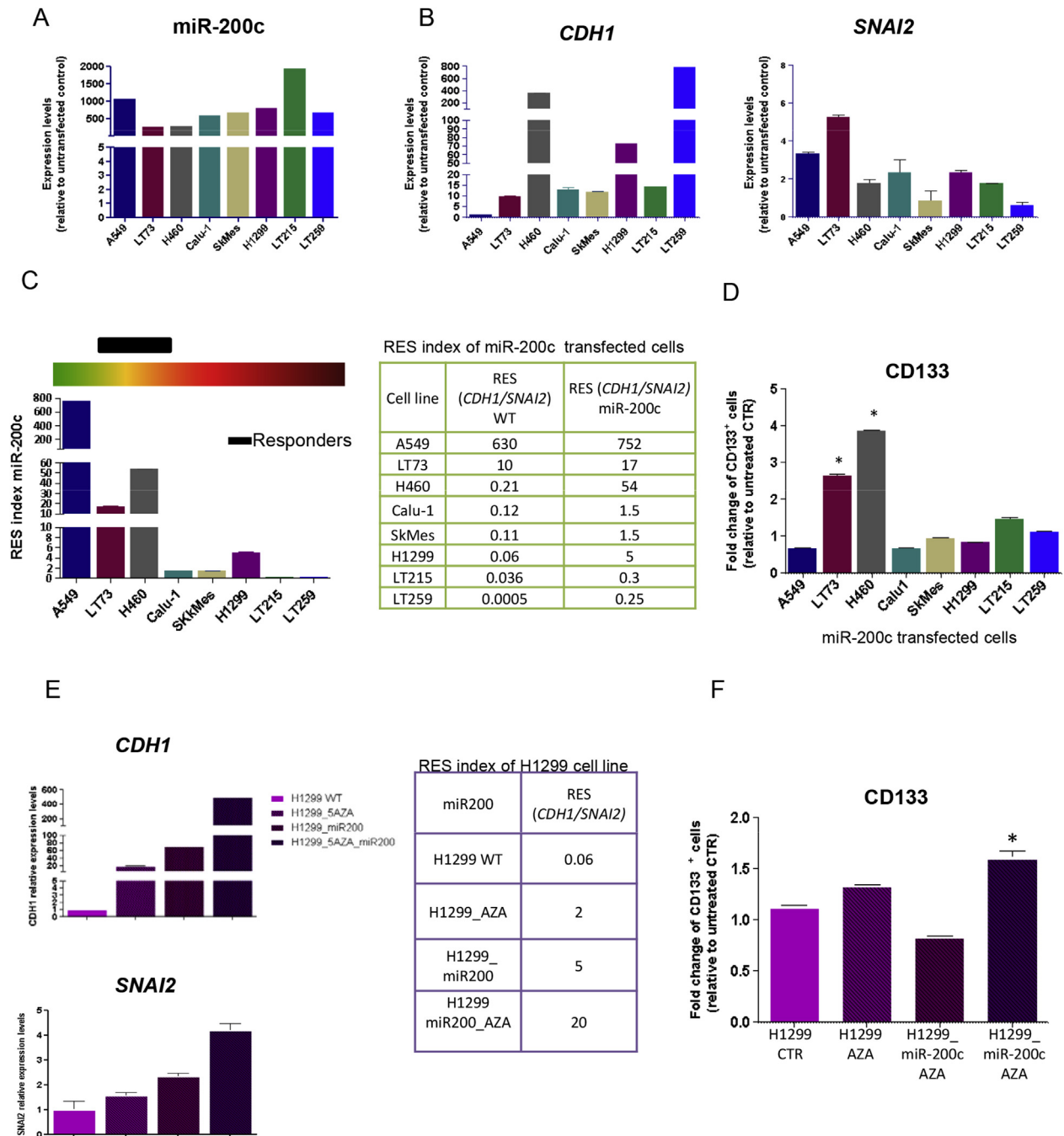ve to scramble transfected cells). RNU48 was used as housekeeping. The data represent two independent transfections each with three replicates and are represented as mean ± SD. **(B)** Quantitative Real-Time PCR analysis of CDH1 and SNAI2 expression levels analyzed relatively to scramble transfected cell lines used as reference. Data are representative of three independent experiments with three replicates each. **(C)** Alignment of miR-200c transfected cells on the basis of RES index classification. **(D)** Fold change of CD133 in miR-200c transfected cells after TGFβ1 treatment relative to scramble transfected untreated cells. Data are the results of three independent experiments expressed as mean ± SD. *p $<$ 0.05. **(E)** Expression levels of *CDH1* analyzed by Real-Time PCR relative to control after 5-aza-2'deoxycytidine treatment, miR-200c or miR-200c + 5-aza-2'deoxycytidine treatment. Real-Time PCR data represent the results of three independent experiments each with three replicates, expressed as mean ± SD. **(F)** Fold change of CD133 in H1299 transfected and/or 5-aza-2'deoxycytidine treated cells after TGFβ1 treatment (relative to untreated cells). Plots represent fold changes ± SD of three independent experiments. *, p $<$ 0.05.
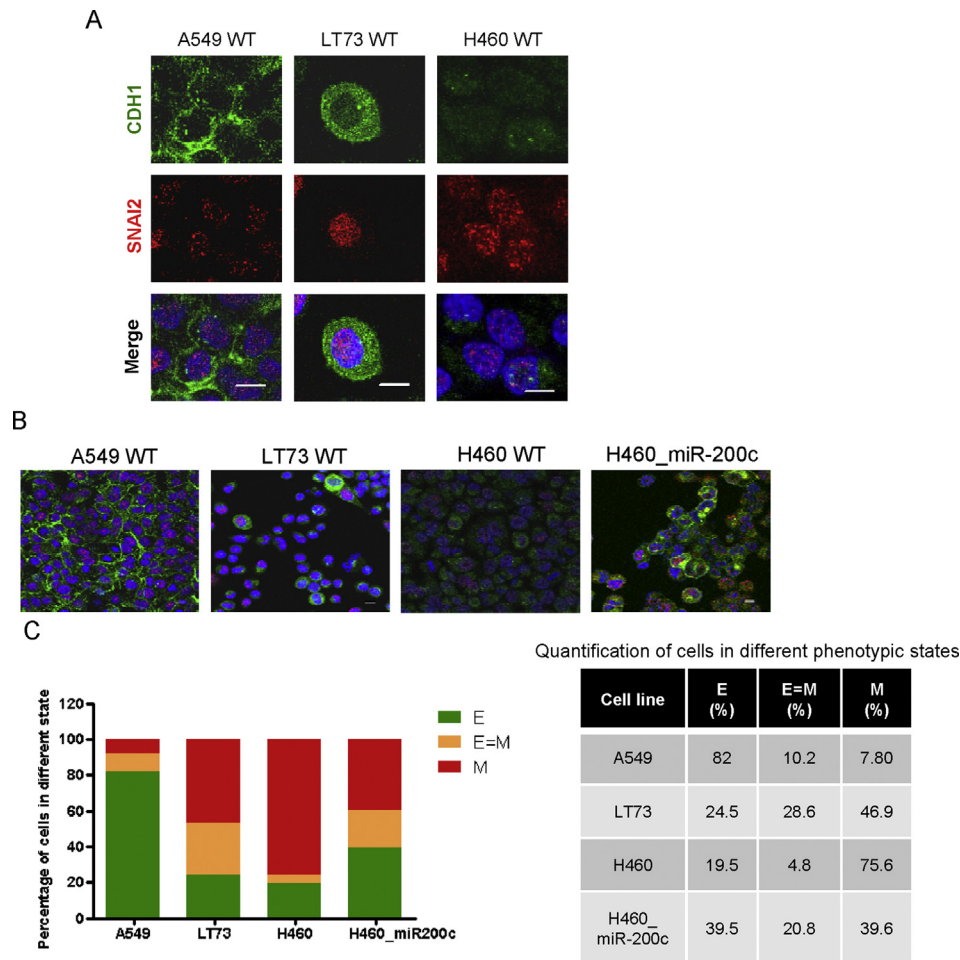
Figure 4 − The frequency of cells co-expressing epithelial and mesenchymal markers defines cellular plasticity. (A,B) Representative immunofluorescence analysis of cells of the different cell lines stained with CDH1 (green) and SNAI2 (red). Images are at 63× (A) and 40× (B) magnification. Scale bar 10 μm. C) Relative percentage of different cell subpopulations in different cell lines calculated with ImageJ software. 100 cells in two independent experiments were counted.

stimulation such as LT73 (E = M 28.5%) or A549 cells which still contained a sizeable percentage of hybrid cells (E = M 10.2%), possibly sufficient to confer to the cell line a plastic behavior (Figure 4C). We also noted a cytoplasmic re-distribution of CDH1 in LT73 cell line. In the basal state, H460 cells, on the contrary, showed low frequency of hybrid cells (E = M, 4.88%) consistent with their weak responsiveness to TGFβ1 (Figure 4C). Interestingly, exogenous expression of miR-200c in H460 cells produced an increase in the double-positive population (E = M, 20.8%), mirrored by acquisition of increased responsiveness to external stimuli (Figures 4B, C and 3D).

3.5. Phenotypic state influences spontaneous de novo formation of CD133^{+} cells

Several observations suggest that non-CICs can convert to CICs, associating the concept of plasticity also to a non-stem cell population. To explore the reason of different response to ME stimuli in cells with different phenotypic states, LT73 (M/E) cells, H460 cells (M^{+}) and their respective miR-200c transfectants were depleted of CD133^{+} CICs by FACS sorting to obtain CD133Negative populations (LT73CD133Neg and

H460CD133Neg cells respectively). The success of sorting procedure was evaluated after 2 days of culture for both LT73 and H460 cell lines and resulted in 85% of CD133^{+} cells depletion. RES index of the LT73CD133Neg cell line was comparable to the LT73 unsorted parental cell line. Interestingly, RES index of sorted CD133 + cells was slightly lower compared to both bulk parental and LT73CD133Neg cell lines due to higher expression of mesenchymal markers, a profile consistent with recently reported lung CICs signatures (Rothwell et al., 2014).

Spontaneous formation of CD133^{+} cells was monitored by flow-cytometry for 28 days, from day 2 to day 30, in absence of ME stimuli in both cell lines. Under standard culture conditions LT73CD133Neg cells remained stable during the observation period, indicating that in absence of external stimuli, cells with hybrid phenotype do not spontaneously generate CD133^{+} cells. Both, LT73CD133Neg cells and LT73CD133Neg_miR-200c as a result of their plastic behavior, efficiently responded to TGFβ1 stimulation in generating CD133^{+} cells (respectively, 0.08 ± 0.008 for LT73CD133Neg, 0.06 ± 0.01 for LT73CD133Neg_miR-200c) indicating quick response to external stimuli (Figure 5A, panels a, b). Conversely,
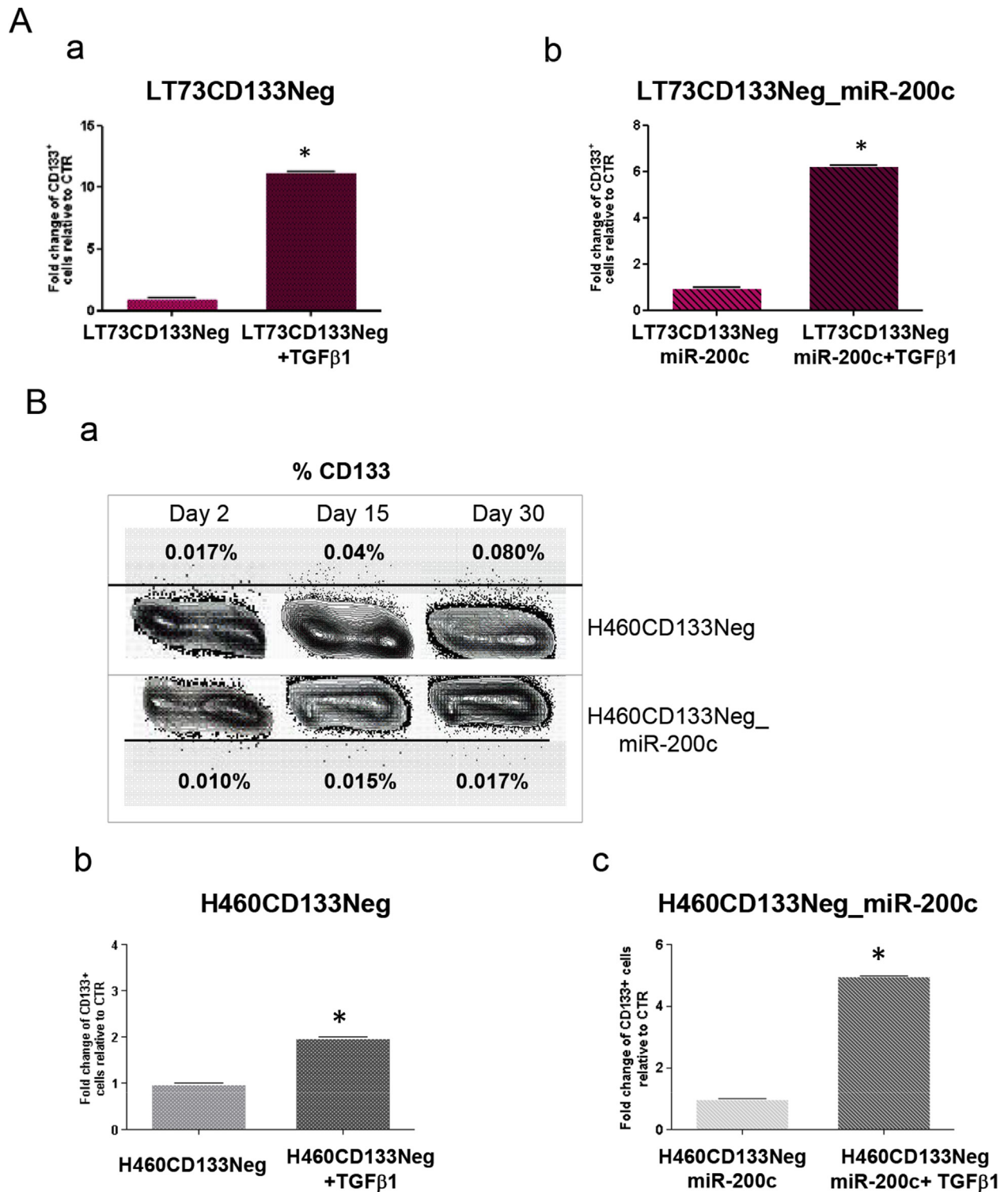
Figure 5 − De novo generation of CD133$^+$ cells in CICs depleted cells. (A) Fold change of CD133$^+$ cells in LT73CD133Neg cells (a) and LT73-CD133Neg_miR-200c cells (b) after TGFβ1 treatment (relative to untreated control). Bars represent three independent experiments mean ± SD. *p < 0.05. (B) Representative result of three independent experiments performed by flow cytometry of spontaneous formation of CD133$^+$ cells in H460CD133Neg or H460CD133Neg_miR-200c after 30 days of *in vitro* culture (a). Fold change of frequency of CD133$^+$ cells in H460CD133Neg (b) cells and H460CD133Neg_miR200 cells (c) after TGFβ1 treatment (relative to untreated control). Bars represent three independent experiments. *p < 0.05.

H460CD133Neg cells generated spontaneously a CD133$^+$ population in culture during time, with a propensity to restore rapidly original phenotypic equilibrium. However, H460CD133Neg cells treated with miR-200c remained negative during time (Figure 5B, panel a), due to the acquired hybrid phenotype. Moreover H460CD133Neg cells under TGFβ1 treatment showed a slight increase of CD133$^+$ (0.02 ± 0.007) cells, indicating inability to integrate ME intervention to create *de novo* CICs (Figure 5B panel b) while H460CD133Neg_miR-200c responded efficiently to TGFβ1 stimulation by generating CD133$^+$ cells (0.05 ± 0.01) (Figure 5B, panel c). To standardize treatments for each cell line, TGFβ1 was added at day 2 after sorting and the cells were collected two days treatment.

3.6. Phenotypic plasticity regulates response to pro-tumorigenic activity of cancer-associated fibroblasts

Stromal cells are increasingly recognized as crucial contributors to cancer formation and progression (Joyce and Pollard, 2009). Among different players in the cancer microenvironment a prominent role is attributed to cancer-associated fibroblasts (CAFs), which have been shown to increase tumorigenicity of different epithelial tumors, including lung cancer (Navab et al., 2011; Orimo and Weinberg, 2006). Stimuli from lung CAFs have also been shown to increase stemness in lung cancer cells (Chen et al., 2014) both through a direct contact or through secretion of different cytokines (including TGFβ1) that are released in a paracrine manner and that regulate their biological behavior.

To verify whether response to physiological cues related to the cancer microenvironment could also be regulated by phenotypic plasticity of hybrid cells, cell lines were first treated with media conditioned (CM) by cancer associated fibroblasts (CAFs) isolated from lung cancer tissue and subsequently subcutaneously injected in nude mice in absence or in presence of CAFs. The treatments with fibroblasts conditioned media (CM, n = 5), showed increased levels of CD133$^+$ cells in cell lines that exhibited a hybrid phenotype, while cells previously shown as unresponsive to TGFβ1 did not respond to stimuli induced by CM (Figure 6A). Additional *in vitro* experiments were also performed to explore whether the paracrine effect of CAFs CM occurred mainly through the TGFβ1 signaling or also through other pathways using TGFβ1 neutralization antibody. The ability of LT73CD133Neg cell line to form CD133$^+$ cells under TGFβ1 or CM treatment was significantly inhibited by TGFβ1 antibody (p = 0.01) however the frequency of CD133$^+$ cells was still statistically different compared with the control group (p = 0.036) indicating that TGFβ1 is not the only signal involved in increasing stemness phenotype (Supplementary Figure 3A). Based on this, we explored another important paracrine signal that has been described to be involved in the maintenance of cancer stemness, IGFII/IGF1R (Chen et al., 2014). LT73CD133Neg cells treated with IGFII recombinant protein or CM showed increased frequency of CD133$^+$ cells (2.65 fold change increase) while the inhibition of IGFII in LT73CD133Neg cells only partially prevented the formation of CD133$^+$ cells (Supplementary Figure 3B). Interestingly the inhibition of both TGFβ1 and IGFII in CM-treated LT73CD133Neg suppressed *de novo* formation of CD133$^+$ cells (Supplementary Figure 3B, C).

To verify that response to stimuli could be regulated by cell plasticity through paracrine mechanisms LT73, H460 parental and H460_miR200c cell lines were injected in nude mice in absence or presence of CAFs. Co-injection with fibroblasts increased tumorigenicity of LT73 cells (n = 32) compared to controls (n = 16) (p < 0.05) (Figure 6B, panel a). Increased frequency of CD133$^+$ cells in co-injected tumors was observed, indicating that microenvironment stimuli can play a critical role in tumor formation by modulating CD133 phenotype (Figure 6B, panel b). Moreover, an increased number of cancer cells, even if not statistically significant likely due to the low number of animals, was detected in the lungs of mice carrying heterotypic tumors (n = 10) (p = 0.05) compared to controls (n = 4) possibly related to the increase of CD133$^+$ cells upon fibroblast modulation (Figure 6B, panel c). Conversely, *in vivo* growth of H460 cells was not affected by fibroblasts co-injection (n = 32) compare to controls (n = 14) (p = 0.08) (Figure 6C, panel a) and the explanted heterotypic tumors did not show increased numbers of CD133$^+$ cells (Figure 6C, panel b). Finally no significant increase in human cancer cells was found in lungs of co-injected mice (n = 4) compared to controls (n = 4) (p = 0.1). (Figure 6C, panel c).

To confirm the possibility that lung cancer cells could become sensitive to microenvironmental stimuli *in vivo* under acquisition of a more plastic phenotype, H460 cells transfected with miR-200c were also injected in absence or in presence of human lung fibroblasts. Tumor growth was increased in H460_miR-200c cells co-injected with fibroblasts (n = 16) compared to controls (n = 16) (Figure 6D, panel a), with concomitant increase of CD133$^+$ cells frequency (Figure 6D, panel b) in tumor xenografts. Enhanced cancer cells in murine lungs of co-injected mice (n = 4) compared to controls alone (n = 4) (p = 0.06) was also detected (Figure 6D, panel c). Overall these results suggest that proclivity to generate CICs under physiological microenvironment stimuli *in vivo* is also controlled by balance between epithelial and mesenchymal features.

3.7. SNAI2 and CDH1 combined expression is associated with poor outcome in lung cancer patients

To evaluate whether presence of a specific pattern of epithelial and mesenchymal markers could stratify tumors with peculiar characteristics of plasticity and could be correlated with clinical outcome, 60 samples from NSCLC patients, with a median follow-up of 24 months, were examined for the expression of CDH1 and SNAI2 by immunohistochemistry (clinical characteristics are reported in Table 1). Different patterns of expression were observed and correlated with previous experimental findings: most cases did not express SNAI2 (62%) and were considered mainly epithelial (E$^+$). Among cases showing SNAI2 immunostaining, analysis of the intracellular staining intensity classified 14 out of 60 cases (23%) as intermediate expressors and 9 out of 60 cases (15%) as high expressors (Figure 7A, panel a). As generally observed in lung cancer, CDH1 was expressed in all primary tumors with a specific staining at membrane level. The evaluation of CDH1 expression pattern was performed considering both, the membrane intensity staining (MI), and the extension of the staining (E) defined as complete or incomplete staining

around the membrane. The intensity of the membrane was evaluated as intermediate (MI = 1, comparable to internal control), or high (MI = 2, higher than internal control), and extension of membrane staining as incomplete (E = 1) or complete (E = 2) (Figure 7A, panel b). Cases were then stratified on the basis of the combined expression between the two markers. In particular, tumors showing a peculiar pattern with balance between the two markers were considered hybrid (E/M, 8.3%). Generally, clinical-pathological characteristics did not directly correlate with tumor phenotypes (epithelial, hybrid or mesenchymal) with the exception of a significant association between squamous histology and mesenchymal tumors (p < 0.01).

We then considered the prognostic implications of CDH1 and SNAI2 expression patterns alone or combined. In the survival analysis, none of the two markers alone (SNAI2 nuclear staining or E-cadherin) was a significant predictor of survival (Figure 7B, panels a, b). We found, instead, a significant reduced survival in patients whose tumors were considered hybrid for epithelial and mesenchymal features (E/M) for their specific pattern, displaying a balance in the expression between the two proteins SNAI2 and CDH1 (n = 5) compared to tumors displaying high epithelial features (n = 47), (p = 0.04). A difference was also found when tumors with hybrid features (E/M) were compared with mesenchymal tumors (M+); this difference however was not significant possibly due to the low number of patients (p = 0.08) (Figure 7B, panel c). Significantly different outcome was also observed when hybrid tumors (E/M) were compared to the other groups (E+ and M+) combined (p = 0.03) (Figure 7B, panel d).

4.   Discussion

Recent data surrounding the plasticity concept provide evidence that the pool of cancer initiating cells may derive from phenotypic switching of progenitors within the tumors both driven by instructive stimuli from the microenvironment or by a spontaneous conversion process (Marjanovic et al., 2013). In the present study we uncover the dynamic connection between microenvironment and cellular plasticity, thus revealing how physiological stimuli could influence the generation and/or maintenance of cancer initiating cells during lung cancer progression.

We initially observed that the efficiency of TGFβ1 in modulating the frequency of CD133+ CICs was heterogeneous in NSCLC cell lines and apparently uncoupled from the induction of the EMT process. Since no apparent correlation was observed with histological subtypes or genetic lesions, we reasoned that the different behavior in generating CD133+ cells under ME stimuli could therefore be more likely associated to the basal phenotypic state of the different cell lines. Interestingly the models showing higher responsiveness to TGFβ1 were those displaying hybrid epithelial/mesenchymal characteristics as determined by the ratio of expression of CDH1 and SNAI2 (RES index). Acknowledging the limitations in the use of only two markers to divide cell lines in different 'phenotypic' groups, we also noticed that the use of multiple markers, while surely providing better precision for classification purposes, is also less amenable to rapid clinical

application, while in this work we also show preliminary data on possible use of these two markers (which also perform robustly in IHC) on FFPE clinical specimens. On the same note the RES index provides good correlation with the plasticity of the cellular models but does not provide perfect 'discrimination' power between responsive and non-responsive models at all values. In particular the relative increase in CD133+ cells observed in H460 (RES 0.21) cells after TGFβ1 stimulation is lower than that observed for A549 (RES 630) and LT73 (RES 10) indicating that H460 cells are probably at the 'border' of plasticity. This observation implies therefore that the RES index could only provide an estimate of response for models with RES between 0 and 5. In this context while H1299_miR200c cells (RES 5) do not respond to TGFβ1, when the CDH1 promoter is de-methylated by 5′AZA treatment, the resulting cells (RES 20) show good response. Consistently when RES index is increased in H460 cells by miR200c transfection (H460_miR200c, RES 54) the ensuing cells show greatly increased response to TGFβ1.

The observed link between plasticity and stemness is in line with recent evidence pointing at a crucial role of dynamic changes between epithelial and mesenchymal phenotypes in dictating cancer progression. In fact, while acquisition of mesenchymal features trough the EMT process has long been associated with some aspects of cancer aggressiveness, the requirement of a tight spatiotemporal regulation of this process, including its reversion in the mesenchymal-to-epithelial transition, has been shown to be crucial for efficient metastasization (Ocana et al., 2012; Tsai et al., 2012). Dynamic changes in epithelial and mesenchymal phenotypes of circulating tumor cells (CTCs) have also been described in breast cancer patients and correlated with clinical outcome highlighting the extreme relevance of cancer cell plasticity (Yu et al., 2013). Interestingly, in the same study, a small number of cells co-expressing mesenchymal and epithelial features was detected in primary breast tumors and in migrating 'clusters' of CTCs with potential connections to metastasis formation (Yu et al., 2013). Hybrid phenotypes could therefore identify tumors with greater ability to 'sense' microenvironment signals and for this reason lung cancer cells displaying both epithelial and mesenchymal traits may retain high level of plasticity and could be highly reactive to convert to stemness state.

Both experimental evidence and mathematical modeling have recently been used to support the hypothesis of the existence of a core decision system regulating EMT and playing an important role as a major determinant of cellular plasticity in association with other important cellular mechanisms such as cell cycle arrest, apoptosis, cell−cell communication and stemness (Brabletz et al., 2011; Brabletz and Brabletz, 2010; Lu et al., 2013). In this network the circuit of miR-200/ZEB is predicted to form a tri-stable state: the epithelial state, with high miR-200 and low ZEB, the mesenchymal state with low miR-200 and high ZEB and a hybrid state, with intermediate level of both miR-200 and ZEB that is the one that is referred to as partial EMT responsible of a collective cell migration and eventually of a reversion to mesenchymal epithelial transition required for the metastatic process (Christiansen and Rajasekaran, 2006). It is tempting to speculate, therefore, that this responsive state could be related to both the
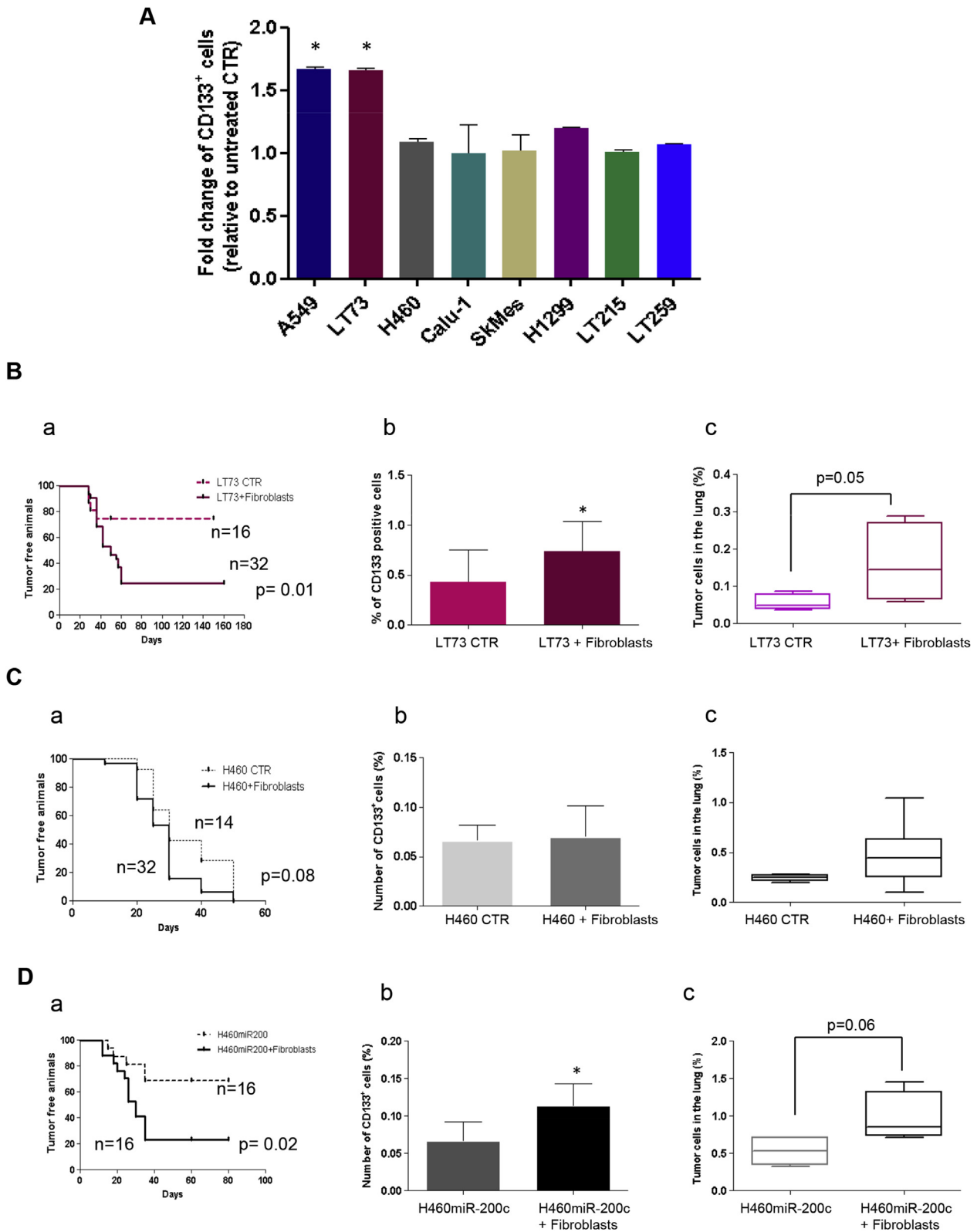
Figure 6 − Microenvironmental stimuli promote selective *in vivo* tumor growth and spread of lung cancer cells with plastic phenotype. (A) Fold change of CD133$^+$ cells in lung cancer cell line treated with five different fibroblasts conditioned media (n = 5). The results are represented as the mean value of CD133$^+$ cells increase after different CM treatments compared to untreated control (±SD) Significant increase was seen only in A549 and LT73 cells (*p < 0.05). (B) (a) Kaplan−Meier curves representing tumor free animals injected with LT73 cells alone (n = 16, dashed line) or co-injected with fibroblasts (n = 32, solid line). p value was calculated using the log-rank test. Statistical significance was set at p < 0.05. (b) Frequency of CD133$^+$ cells is significantly different between tumors originated from LT73 alone or co-injected with fibroblasts. The results are expressed as the mean ± SD of frequency of CD133$^+$ cells in control xenografts and co-injected xenografts. *p < 0.05 was calculated with

|	No of patients (%)	Epithelial (%)	p-value	Hybrid (%)	p-value	Mesenchymal (%)	p-value
Table 1 – Correlation between tumors phenotype and clinico-pathological characteristics of 60 NSCLC patients.							
Gender			1.000		1.000		1.000
Male	46 (76.6)	36 (76.5)		4 (80)		6 (75)	
Female	14 (23.3)	11 (23.4)		1 (20)		2 (25)	
Age			1.000		0.64		0.700
≤70	24 (40)	19 (40.4)		3 (60)		2 (25)	
>70	36 (60)	28 (59.5)		2 (40)		6 (75)	
Histology*			0.094		0.148		0.001
ADC	38 (63.3)	37 (78.7%)		1 (20)		0 (0)	
SCC	12 (20)	2 (4.3%)		2 (40)		8 (100)	
Others	10 (16.6)	8 (17%)		2 (40)		0 (0)	
Stage**			0.287		1.000		0.402
IA–IB	24 (40)	18 (39.1)		3 (60)		3 (50)	
IIA–IIB	11 (18.3)	9 (19.5)		0 (0)		2 (33.3)	
IIIA	20 (33.3)	17 (36.9)		2 (40)		1 (16.6)	
IV	2 (3.3)	2 (4.3)		0 (0)		0 (0)	
Smoking Status			0.827		0.351		1.000
Smokers	23 (38.3)	16 (43.3)		4 (80)		3 (42.8)	
Former	26 (43.3)	21 (56.7)		1 (20)		4 (57.2)	

*(ADC vs.SCC + others)**(Stage I–II vs. Others).

intermediate RES index (for the bulk cell populations) and the frequency of CDH1/SNAI2 double-positive cells (at single cell level) identified in the present study as related to tendency to form CICs in response to external cues.

New lines of evidence suggest that a tight specific epigenetic regulation represents an important determinant in controlling genes associated with the EMT process and that specific chromatin configuration associated with the promoter of the EMT-inducing factor ZEB1 (Chaffer et al., 2013) and more recently to SNAI2 (Phillips et al., 2014) affects the cell-state transition and formation of cancer initiating cells. Only plastic non-CSCs maintain the ZEB1 promoter in a bivalent chromatin configuration, enabling them to respond readily to microenvironmental signals. In response to ME, the ZEB1 promoter converts from a bivalent to active chromatin configuration, ZEB1 transcription increases, and non-CSCs subsequently enter the CSC state thereby increasing the aggressiveness and tumorigenic potential (Chaffer et al., 2013). In our study modulating the balance between epithelial and mesenchymal features with miR-200c changed cellular phenotype allowing rapid generation of CD133^{+}CICs cells

from previously unresponsive models and also suggesting the extreme relevance of epigenetic control in dictating cell-state changes. It has been also demonstrated that the epigenetic silencing of CDH1 promoter by methylation confers full mesenchymal traits to cancer cells (Maruyama et al., 2011; Phillips et al., 2014). In this study we have used H1299 cell line, originated from a lung cancer metastatic lymphnode, which has a highly methylated CDH1 promoter. The epigenetic treatment with 5-aza-2'-deocxycytidine-demethylating agent partially restored the expression of CDH1. However for this particular model the re-expression of CDH1 was not sufficient to allow the shift of cells from mesenchymal to plastic state, and same results were obtained with cells transfected with miR-200c. When cells were treated with 5-aza-2'deoxycytidine and miR-200c a synergic effect with a concomitant change in phenotypic state, response to ME and creation of stemness phenotype was obtained. A possible explanation of this behavior is that transcriptional silencing of CDH1 besides hyper-methylation of its promoter may be ascribed to the presence of ZEB1-histone deacetylase repressor on CDH1 promoter. miR-200c inhibits class III histone deacetylase silent

Student's t. (c) Percentage of human cancer cells detected in the lungs of mice carrying co-injected tumors (n = 10) compared to control mice (n = 4) (p = 0.05). The data represent the mean of percentage of human cells ± SD. p value was calculated with Student's t. (C) (a) Kaplan−Meier curves representing tumor free animals injected with H460 cells alone (n = 14, dashed line) or co-injected with fibroblasts (n = 32, solid line). p value was calculated using the log-rank test. Statistical significance was set at p < 0.05. (b) Frequency of CD133^{+} cells is not significantly different between xenografts obtained from H460 cells injected alone or co-injected with fibroblasts. The results are expressed as mean ± SD. p value was calculated with Student's t. (c) Percentage of human cancer cells detected in the lungs of mice carrying co-injected tumors (n = 4) is not different compared to control mice (n = 4) (p = 0.1). The data represent the mean of percentage of human cells ± SD. p value was calculated with Student's t. (D) (a) Kaplan−Meier curves representing tumor free animals injected with H460_miR-200c cells alone (n = 16, dashed line) or co-injected with fibroblasts (n = 16, solid line). Difference between curves is significant with an increased number of events in co-injected cells p = 0.02. p value was calculated using the log-rank test. (b) Frequency of CD133^{+} cells is significantly different between xenografts from H460_miR-200c, alone or co-injected with fibroblasts. *p < 0.05 was calculated with Student's t.The results were expressed as the mean ± DS. p value was calculated with Student's t (c) Percentage of human cancer cells detected in the lungs of mice carrying co-injected tumors (n = 4) compared to control mice (n = 4) (p = 0.06). p value was calculated with Student's t.
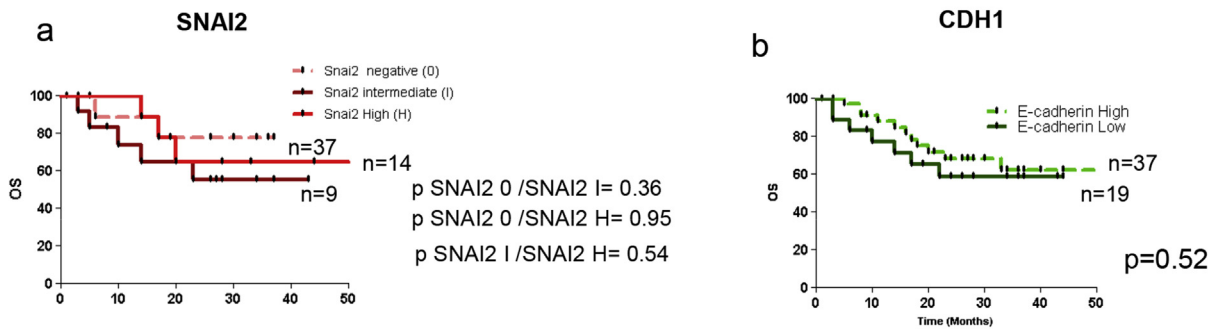
A

a   SNAI2

b   CDH1
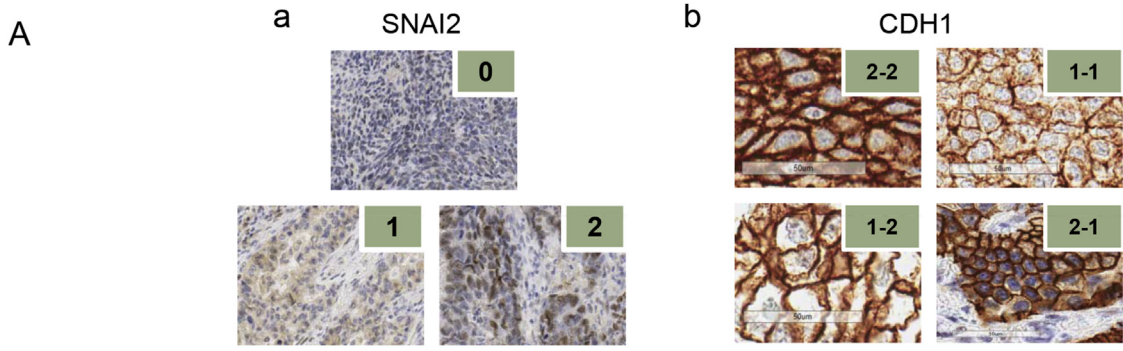
c

🟩 CDH1 high   🟨 CDH1or SNAI2 intermediate   🟥 SNAI2 high

N of patients	STATE	GROUPS			
	Phenotype	SNAI2	CDH1 (MI)	CDH1(E)	
37	E+	0	1-2	1-2	
4	E+	1	2	2	
6	E+	1	2	1	
1	E>M	1	1	2	
3	E=M	1	1	1	
1	M=E	2	2	1	
0	M>E	2	1	2	
4	M+	2	1	1	
4	M+/E+	2	2	2	

Stratification of lung cancer patients by tumors phenotypic state

B

a   SNAI2

p SNAI2 0 /SNAI2 I= 0.36
p SNAI2 0 /SNAI2 H= 0.95
p SNAI2 I /SNAI2 H= 0.54

b   CDH1

p=0.52

Combined

c

* p E/M vs E+= **0.04**
p E/M vs M+= **0.08**
p E+vs M+= 0.62

d

*p=0.03
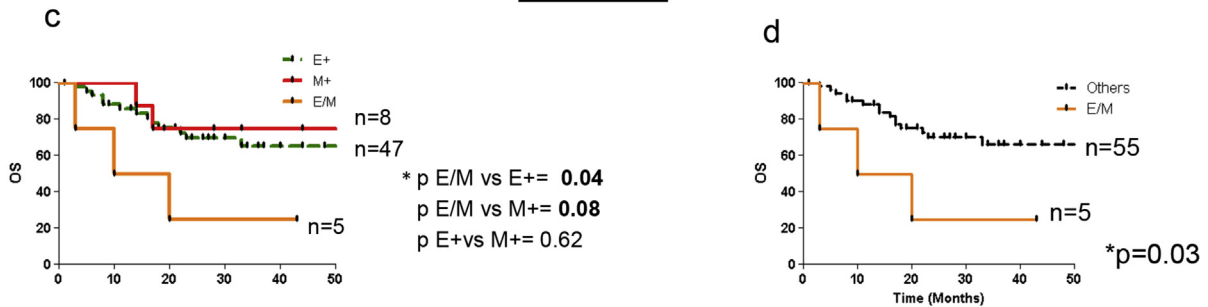
information regulator 1 (SIRT1), resulting in a re-expression of epigenetically silenced CDH1 thus the concomitant treatment with de-methylating agent and miR-200c that is expected to increased histone acetylation (Tryndyak et al., 2010) allowed cells to re-express CDH1 adequately for a shift into plastic state.

To better comprehend progenitor cells dynamics in cancer cells of different phenotype in relation to ME stimuli we also used CICs depleted models, LT73CD133Neg and H460CD133Neg. Our results are in line with recently published data reporting de novo creation of cancer initiating cells under ME stimuli (Gupta et al., 2011; Mani et al., 2008; Scheel et al., 2011). Long-term culturing highlighted the fact that in the more mesenchymal cells (H460CD133Neg) there was the propensity to "spontaneous" conversion of CD133-cells to CD133$^+$ cells leading to restoration of the initial content of CICs. This could be likely ascribed to activation of an autocrine mechanism and indicates again lesser propensity to communication with different cells. While in vitro, this phenotype could be associated with reconstitution of CICs content, it is likely that in vivo, the increased tumorigenesis and cells dissemination could be linked to plasticity and ability to integrate different environmental cues as demonstrated by the loss of metastatic potential of cells 'locked' into full mesenchymal state (Tsai et al., 2012). LT73CD133Neg or H460CD133Neg transfected with miR-200c remained steadily negative in culture conditions during the same period of time in accordance to the acquired ME 'responsive' phenotype. Upon exposure to TGFβ1 both cell lines quickly responded to microenvironmental stimuli and de novo formation of CD133$^+$ cells was observed. This plasticity is likely controlled by paracrine mechanisms as suggested also for pro-tumorigenic activity of cancer-associated fibroblasts (Bertolini et al., 2015; Chen et al., 2014).

We could therefore speculate that the small subpopulation of cells co-expressing both epithelial and mesenchymal markers could be the one that has the capability to sense the ME stimuli and able to generate CD133$^+$ cells. Interestingly in LT73 we also observed a cytoplasmic redistribution of the CDH1 that may reflect a partial loss of adhesion functionality (Nawrocki-Raby et al., 2003). Further studies are warranted to investigate this hypothesis.

Since identifying molecular markers to distinguish resectable NSCLC patients with a high risk of recurrence is essential to improving therapeutic outcome, we reasoned that also in primary human tumors contribution from microenvironment could be crucial. In this respect tumors endowed with plasticity (i.e. showing a balance between epithelial and mesenchymal properties) could have an advantage for metastasization even compared to tumors with exclusive mesenchymal features. In fact, interesting studies highlighted both the implication of a reversible EMT process as key driving force in human carcinoma metastasis and the fact that tumor dormancy could be related to the inability of disseminated tumor cells, locked in an irreversible mesenchymal state, to revert EMT and proliferate (Celia-Terrassa et al., 2012; Tsai et al., 2012). Here we analyzed a cohort of 60 NSCLC cases and show that a specific combined pattern of CDH1 and SNAI2 expression may represents an important disease prognosticator, possibly identifying more plastic tumors with worse prognosis. Moreover our results are in accordance with a relatively recent study (Kase et al., 2000) that assessed that CDH1 was not an independent prognostic marker of the disease while adequate studies for SNAI2 as a predictor marker are still unavailable. This clinical association suggests that SNAI2 and CDH1 proteins cannot represent prognostic indicators when analyzed independently, however the two markers combined in specific pattern could provide prognostic information about plasticity of tumors more dependent on microenvironment stimuli and identify patients at high risk of poor prognosis. Our data support the concept that the two major genes involved in the EMT process, CDH1 and SNAI2 play a critical role in "tagging" the phenotypic state of lung cancer cells and affect the creation of cells with cancer initiating cells properties under appropriate stimuli derived from microenvironment.

In line with our results, recent work reported that a signature enriched in citoskeletal proteins, identified in aggressive cells with hybrid epithelial/mesenchymal phenotype, is associated with poor prognosis in lung adenocarcinoma patients (Schliekelman et al., 2015). Further studies using a large patient's population and possibly the combination of more epithelial and mesenchymal markers will be required to improve the clinical significance of our findings.

In conclusion the results of our study delineate that changes in cell state and acquisition of stemness properties could be controlled at single cell level by regulation of expression of mesenchymal and epithelial markers regulating cellular plasticity. These findings open possibilities to better understand the causes and the consequences of cell-state transitions in lung cancer cells under microenvironment stimuli with possible implications for therapeutic targeting of CICs inducing signals. Investigation of clinical series will however be required to fully elucidate the complex interactions between cellular phenotypes and microenvironment cues.

Figure 7 – Specific pattern of CDH1 and SNAI2 immunostaining correlates with clinical outcome in lung cancer patients. (A) (a) Representative images of lung cancer sections stained with anti-SNAI2 (negative, intermediate = 1 or high = 2) or (b) anti-E-cadherin (Low, MI = 1 E = 1, intermediate MI = 1 E = 2, MI = 2, E = 1, High MI = 2, E = 2). Scale bar 50 μm (magnification 40×). (c) Stratification of patients by tumor phenotypic state. (B) (a) Kaplan–Meier analysis of overall survival (OS) for patients stratified by negative (0), intermediate (I) or high (H) intensity of SNAI2. (b) Kaplan–Meier analysis of OS for patients stratified by low or high membrane intensity of E-cadherin. (c) Kaplan–Meier curves of patients stratified by phenotypic states (E+,M+ or E/M) of tumors classified by the combination of SNAI2 and CDH1 scores. The colored bars indicate the high expression levels (SNAI2 High = Red M$^+$, CDH1 High = Green E$^+$) or intermediate expression levels (SNAI2 or CDH1 = Yellow E/M) of each marker. (d) Kaplan–Meier curves of patients with plastic phenotype tumors (hybrid E/M) vs. others phenotypic states (E+ and M+). p values were calculated using the log-rank test and are indicated and statistical significance was set at p < 0.05.

Acknowledgments

Appendix A.
Supplementary data

Supplementary data related to this article can be found at http://dx.doi.org/10.1016/j.molonc.2015.10.002.

R E F E R E N C E S

Bertolini, G., D'Amico, L., Moro, M., Landoni, E., Perego, P., Miceli, R., Gatti, L., Andriani, F., Wong, D., Caserini, R., Tortoreto, M., Milione, M., Ferracini, R., Mariani, L., Pastorino, U., Roato, I., Sozzi, G., Roz, L., 2015. Microenvironment-modulated metastatic CD133+/CXCR4+/EpCAM- lung cancer-initiating cells sustain tumor dissemination and correlate with poor prognosis. Cancer Res. 75, 3636−3649.

Bertolini, G., Roz, L., Perego, P., Tortoreto, M., Fontanella, E., Gatti, L., Pratesi, G., Fabbri, A., Andriani, F., Tinelli, S., Roz, E., Caserini, R., Lo Vullo, S., Camerini, T., Mariani, L., Delia, D., Calabro, E., Pastorino, U., Sozzi, G., 2009. Highly tumorigenic lung cancer CD133+ cells display stem-like features and are spared by cisplatin treatment. Proc. Natl. Acad. Sci. U. S. A 106, 16281−16286.

Brabletz, S., Bajdak, K., Meidhof, S., Burk, U., Niedermann, G., Firat, E., Wellner, U., Dimmler, A., Faller, G., Schubert, J., Brabletz, T., 2011. The ZEB1/miR-200 feedback loop controls notch signalling in cancer cells. EMBO J. 30, 770−782.

Brabletz, S., Brabletz, T., 2010. The ZEB/miR-200 feedback loop−a motor of cellular plasticity in development and cancer? EMBO Rep. 11, 670−677.

Burrell, R.A., McGranahan, N., Bartek, J., Swanton, C., 2013. The causes and consequences of genetic heterogeneity in cancer evolution. Nature 501, 338−345.

Celia-Terrassa, T., Meca-Cortes, O., Mateo, F., de Paz, A.M., Rubio, N., rnal-Estape, A., Ell, B.J., Bermudo, R., Diaz, A., Guerra-Rebollo, M., Lozano, J.J., Estaras, C., Ulloa, C., varez-Simon, D., Mila, J., Vilella, R., Paciucci, R., Martinez-Balbas, M., de Herreros, A.G., Gomis, R.R., Kang, Y., Blanco, J., Fernandez, P.L., Thomson, T.M., 2012. Epithelial-mesenchymal transition can suppress major attributes of human epithelial tumor-initiating cells. J. Clin. Invest 122, 1849−1868.

Ceppi, P., Mudduluru, G., Kumarswamy, R., Rapa, I., Scagliotti, G.V., Papotti, M., Allgayer, H., 2010. Loss of miR-200c expression induces an aggressive, invasive, and chemoresistant phenotype in non-small cell lung cancer. Mol. Cancer Res. 8, 1207−1216.

Chaffer, C.L., Brueckmann, I., Scheel, C., Kaestli, A.J., Wiggins, P.A., Rodrigues, L.O., Brooks, M., Reinhardt, F., Su, Y., Polyak, K., Arendt, L.M., Kuperwasser, C., Bierie, B., Weinberg, R.A., 2011. Normal and neoplastic nonstem cells

can spontaneously convert to a stem-like state. Proc. Natl. Acad. Sci. U. S. A 108, 7950−7955.

Chaffer, C.L., Marjanovic, N.D., Lee, T., Bell, G., Kleer, C.G., Reinhardt, F., D'Alessio, A.C., Young, R.A., Weinberg, R.A., 2013. Poised chromatin at the ZEB1 promoter enables breast cancer cell plasticity and enhances tumorigenicity. Cell 154, 61−74.

Chen, W.J., Ho, C.C., Chang, Y.L., Chen, H.Y., Lin, C.A., Ling, T.Y., Yu, S.L., Yuan, S.S., Chen, Y.J., Lin, C.Y., Pan, S.H., Chou, H.Y., Chen, Y.J., Chang, G.C., Chu, W.C., Lee, Y.M., Lee, J.Y., Lee, P.J., Li, K.C., Chen, H.W., Yang, P.C., 2014. Cancer-associated fibroblasts regulate the plasticity of lung cancer stemness via paracrine signalling. Nat. Commun. 5, 3472.

Christiansen, J.J., Rajasekaran, A.K., 2006. Reassessing epithelial to mesenchymal transition as a prerequisite for carcinoma invasion and metastasis. Cancer Res. 66, 8319−8326.

Cieslik, M., Hoang, S.A., Baranova, N., Chodaparambil, S., Kumar, M., Allison, D.F., Xu, X., Wamsley, J.J., Gray, L., Jones, D.R., Mayo, M.W., Bekiranov, S., 2013. Epigenetic coordination of signaling pathways during the epithelial-mesenchymal transition. Epigenetics. Chromatin 6, 28.

Easwaran, H., Tsai, H.C., Baylin, S.B., 2014. Cancer epigenetics: tumor heterogeneity, plasticity of stem-like states, and drug resistance. Mol. Cell 54, 716−727.

Eramo, A., Lotti, F., Sette, G., Pilozzi, E., Biffoni, M., Di Virgilio, A., Conticello, C., Ruco, L., Peschle, C., De Maria, R., 2008. Identification and expansion of the tumorigenic lung cancer stem cell population. Cell Death Differ 15, 504−514.

Gonzalez, D.M., Medici, D., 2014. Signaling mechanisms of the epithelial-mesenchymal transition. Sci. Signal 7, re8.

Gregory, P.A., Bert, A.G., Paterson, E.L., Barry, S.C., Tsykin, A., Farshid, G., Vadas, M.A., Khew-Goodall, Y., Goodall, G.J., 2008. The miR-200 family and miR-205 regulate epithelial to mesenchymal transition by targeting ZEB1 and SIP1. Nat. Cell Biol 10, 593−601.

Gupta, P.B., Fillmore, C.M., Jiang, G., Shapira, S.D., Tao, K., Kuperwasser, C., Lander, E.S., 2011. Stochastic state transitions give rise to phenotypic equilibrium in populations of cancer cells. Cell 146, 633−644.

Hanahan, D., Coussens, L.M., 2012. Accessories to the crime: functions of cells recruited to the tumor microenvironment. Cancer Cell 21, 309−322.

Hu, Y., Smyth, G.K., 2009. ELDA: extreme limiting dilution analysis for comparing depleted and enriched populations in stem cell and other assays. J. Immunol. Methods 347, 70−78.

Joyce, J.A., Pollard, J.W., 2009. Microenvironmental regulation of metastasis. Nat. Rev. Cancer 9, 239−252.

Kase, S., Sugio, K., Yamazaki, K., Okamoto, T., Yano, T., Sugimachi, K., 2000. Expression of E-cadherin and beta-catenin in human non-small cell lung cancer and the clinical significance. Clin. Cancer Res. 6, 4789−4796.

Korpal, M., Lee, E.S., Hu, G., Kang, Y., 2008. The miR-200 family inhibits epithelial-mesenchymal transition and cancer cell migration by direct targeting of E-cadherin transcriptional repressors ZEB1 and ZEB2. J. Biol. Chem. 283, 14910−14914.

Kreso, A., Dick, J.E., 2014. Evolution of the cancer stem cell model. Cell Stem Cell 14, 275−291.

Lamouille, S., Xu, J., Derynck, R., 2014. Molecular mechanisms of epithelial-mesenchymal transition. Nat. Rev. Mol. Cell Biol 15, 178−196.

Lim, Y.Y., Wright, J.A., Attema, J.L., Gregory, P.A., Bert, A.G., Smith, E., Thomas, D., Lopez, A.F., Drew, P.A., Khew-Goodall, Y., Goodall, G.J., 2013. Epigenetic modulation of the miR-200 family is associated with transition to a breast cancer stem-cell-like state. J. Cell Sci 126, 2256−2266.

Lu, M., Jolly, M.K., Levine, H., Onuchic, J.N., Ben-Jacob, E., 2013. MicroRNA-based regulation of epithelial-hybrid-

mesenchymal fate determination. Proc. Natl. Acad. Sci. U. S. A 110, 18144–18149.

Mani, S.A., Guo, W., Liao, M.J., Eaton, E.N., Ayyanan, A., Zhou, A.Y., Brooks, M., Reinhard, F., Zhang, C.C., Shipitsin, M., Campbell, L.L., Polyak, K., Brisken, C., Yang, J., Weinberg, R.A., 2008. The epithelial-mesenchymal transition generates cells with properties of stem cells. Cell 133, 704–715.

Marjanovic, N.D., Weinberg, R.A., Chaffer, C.L., 2013. Poised with purpose: cell plasticity enhances tumorigenicity. Cell Cycle 12, 2713–2714.

Maruyama, R., Choudhury, S., Kowalczyk, A., Bessarabova, M., Beresford-Smith, B., Conway, T., Kaspi, A., Wu, Z., Nikolskaya, T., Merino, V.F., Lo, P.K., Liu, X.S., Nikolsky, Y., Sukumar, S., Haviv, I., Polyak, K., 2011. Epigenetic regulation of cell type-specific expression patterns in the human mammary epithelium. PLoS Genet. 7, e1001369.

Meacham, C.E., Morrison, S.J., 2013. Tumour heterogeneity and cancer cell plasticity. Nature 501, 328–337.

Mueller, M.T., Hermann, P.C., Heeschen, C., 2010. Cancer stem cells as new therapeutic target to prevent tumour progression and metastasis. Front Biosci. 2, 602–613 (Elite. Ed).

Navab, R., Strumpf, D., Bandarchi, B., Zhu, C.Q., Pintilie, M., Ramnarine, V.R., Ibrahimov, E., Radulovich, N., Leung, L., Barczyk, M., Panchal, D., To, C., Yun, J.J., Der, S., Shepherd, F.A., Jurisica, I., Tsao, M.S., 2011. Prognostic gene-expression signature of carcinoma-associated fibroblasts in non-small cell lung cancer. Proc. Natl. Acad. Sci. U. S. A 108, 7160–7165.

Nawrocki-Raby, B., Gilles, C., Polette, M., Martinella-Catusse, C., Bonnet, N., Puchelle, E., Foidart, J.M., Van, R.F., Birembaut, P., 2003. E-Cadherin mediates MMP down-regulation in highly invasive bronchial tumor cells. Am. J. Pathol. 163, 653–661.

Ocana, O.H., Corcoles, R., Fabra, A., Moreno-Bueno, G., Acloque, H., Vega, S., Barrallo-Gimeno, A., Cano, A., Nieto, M.A., 2012. Metastatic colonization requires the repression of the epithelial-mesenchymal transition inducer Prrx1. Cancer Cell 22, 709–724.

Orimo, A., Weinberg, R.A., 2006. Stromal fibroblasts in cancer: a novel tumor-promoting cell type. Cell Cycle 5, 1597–1601.

Peinado, H., Olmeda, D., Cano, A., 2007. Snail, Zeb and bHLH factors in tumour progression: an alliance against the epithelial phenotype? Nat. Rev. Cancer 7, 415–428.

Phillips, S., Prat, A., Sedic, M., Proia, T., Wronski, A., Mazumdar, S., Skibinski, A., Shirley, S.H., Perou, C.M., Gill, G., Gupta, P.B., Kuperwasser, C., 2014. Cell-state transitions regulated by SLUG are critical for tissue regeneration and tumor initiation. Stem Cell Rep. 2, 633–647.

Pirozzi, G., Tirino, V., Camerlingo, R., Franco, R., La, R.A., Liguori, E., Martucci, N., Paino, F., Normanno, N., Rocco, G., 2011. Epithelial to mesenchymal transition by TGFbeta-1 induction increases stemness characteristics in primary non small cell lung cancer cell line. PLoS One 6, e21548.

Polyak, K., Weinberg, R.A., 2009. Transitions between epithelial and mesenchymal states: acquisition of malignant and stem cell traits. Nat. Rev. Cancer 9, 265–273.

Rothwell, D.G., Li, Y., Ayub, M., Tate, C., Newton, G., Hey, Y., Carter, L., Faulkner, S., Moro, M., Pepper, S., Miller, C., Blackhall, F., Bertolini, G., Roz, L., Dive, C., Brady, G., 2014. Evaluation and validation of a robust single cell RNA-amplification protocol through transcriptional profiling of enriched lung cancer initiating cells. BMC Genomics 15, 1129.

Scheel, C., Eaton, E.N., Li, S.H., Chaffer, C.L., Reinhardt, F., Kah, K.J., Bell, G., Guo, W., Rubin, J., Richardson, A.L., Weinberg, R.A., 2011. Paracrine and autocrine signals induce and maintain mesenchymal and stem cell states in the breast. Cell 145, 926–940.

Schliekelman, M.J., Taguchi, A., Zhu, J., Dai, X., Rodriguez, J., Celiktas, M., Zhang, Q., Chin, A., Wong, C.H., Wang, H., McFerrin, L., Selamat, S.A., Yang, C., Kroh, E.M., Garg, K.S., Behrens, C., Gazdar, A.F., Laird-Offringa, I.A., Tewari, M., Wistuba, I.I., Thiery, J.P., Hanash, S.M., 2015. Molecular portraits of epithelial, mesenchymal, and hybrid states in lung adenocarcinoma and their relevance to survival. Cancer Res. 75, 1789–1800.

Shih, J.Y., Yang, P.C., 2011. The EMT regulator slug and lung carcinogenesis. Carcinogenesis 32, 1299–1304.

Suzuki, M., Sunaga, N., Shames, D.S., Toyooka, S., Gazdar, A.F., Minna, J.D., 2004. RNA interference-mediated knockdown of DNA methyltransferase 1 leads to promoter demethylation and gene re-expression in human lung and breast cancer cells. Cancer Res. 64, 3137–3143.

Tam, W.L., Weinberg, R.A., 2013. The epigenetics of epithelial-mesenchymal plasticity in cancer. Nat. Med. 19, 1438–1449.

Thiery, J.P., Acloque, H., Huang, R.Y., Nieto, M.A., 2009. Epithelial-mesenchymal transitions in development and disease. Cell 139, 871–890.

Tryndyak, V.P., Beland, F.A., Pogribny, I.P., 2010. E-cadherin transcriptional down-regulation by epigenetic and microRNA-200 family alterations is related to mesenchymal and drug-resistant phenotypes in human breast cancer cells. Int. J. Cancer 126, 2575–2583.

Tsai, J.H., Donaher, J.L., Murphy, D.A., Chau, S., Yang, J., 2012. Spatiotemporal regulation of epithelial-mesenchymal transition is essential for squamous cell carcinoma metastasis. Cancer Cell 22, 725–736.

Visvader, J.E., Lindeman, G.J., 2008. Cancer stem cells in solid tumours: accumulating evidence and unresolved questions. Nat. Rev. Cancer 8, 755–768.

Yu, M., Bardia, A., Wittner, B.S., Stott, S.L., Smas, M.E., Ting, D.T., Isakoff, S.J., Ciciliano, J.C., Wells, M.N., Shah, A.M., Concannon, K.F., Donaldson, M.C., Sequist, L.V., Brachtel, E., Sgroi, D., Baselga, J., Ramaswamy, S., Toner, M., Haber, D.A., Maheswaran, S., 2013. Circulating breast tumor cells exhibit dynamic changes in epithelial and mesenchymal composition. Science 339, 580–584.

Zhou, B.B., Zhang, H., Damelin, M., Geles, K.G., Grindley, J.C., Dirks, P.B., 2009. Tumour-initiating cells: challenges and opportunities for anticancer drug discovery. Nat. Rev. Drug Discov. 8, 806–823.